Earthquakes and Structures, *Vol. 10, No. 4 (2016) 939-963*
DOI: http://dx.doi.org/10.12989/eas.2016.10.4.939

Seismic vulnerability of reinforced concrete building structures founded on an XPS layer

David Koren[a] and Vojko Kilar[*]

Faculty of Architecture, University of Ljubljana, Zoisova 12, SI-1000 Ljubljana, Slovenia

(Received May 5, 2015, Revised December 18, 2015, Accepted December 23, 2015)

Abstract. According to the new directives about the rational and efficient use of energy, thermal bridges in buildings have to be avoided, and the thermal insulation (TI) layer should run without interruptions all around the building - even under its foundations. The paper deals with the seismic response of multi-storeyed reinforced concrete (RC) frame building structures founded on an extruded polystyrene (XPS) layer placed beneath the foundation slab. The purpose of the paper is to elucidate the problem of buildings founded on a TI layer from the seismic resistance point of view, to assess the seismic behaviour of such buildings, and to search for the critical parameters which can affect the structural and XPS layer response. Nonlinear dynamic and static analyses were performed, and the seismic response of fixed-base (FB) and thermally insulated (TI) variants of nonlinear RC building models were compared. Soil-structure interaction was also taken into account for different types of soil. The results showed that the use of a TI layer beneath the foundation slab of a superstructure generally induces a higher peak response compared to that of a corresponding system without TI beneath the foundation slab. In the case of stiff structures located on firm soil, amplification of the response might be substantial and could result in exceedance of the superstructure's moment-rotation plastic hinge capacities or allowable lateral roof and interstorey drift displacements. In the case of heavier, slenderer, and higher buildings subjected to stronger seismic excitations, the overall response is governed by the rocking mode of oscillation, and as a consequence the compressive strength of the XPS could be insufficient. On the other hand, in the case of low-rise and light-weight buildings, the friction capacity between the layers of the applied TI foundation set might be exceeded so that sliding could occur.

Keywords: foundation on thermal insulation; extruded polystyrene (XPS); seismic response; RC structure; soil-structure interaction; nonlinear seismic analysis

1. Introduction

In recent years, the application of low-energy and passive house standards (Feist 1996, 2007, Dequaire 2012, Kuzman *et al*. 2013, Praznik *et al*. 2013, Proietti *et al*. 2013), which began in seismically inactive areas (Northern and Middle Europe), has been slowly gaining ground in earthquake-prone countries (such as Spain, Italy, Greece, Croatia, and Slovenia). Answers to the

*Corresponding author, Professor, E-mail: vojko.kilar@fa.uni-lj.si
[a]Assistant Professor, E-mail: david.koren@fa.uni-lj.si

http://www.techno-press.com/journals/eas&subpage=7 ISSN: 2092-7614 (Print), 2092-7622 (Online)

most common questions related to passive houses can be found in the scientific literature. In order to achieve low energy consumption, passive houses must have a well isolated and air-tight envelope, without thermal bridges. The requirement that buildings should be constructed without thermal bridges is a trend which applies to most newly built buildings. For this reason attempts are frequently made to resolve the question of problematic joints by the insertion of thermally insulating parts between the load-bearing structural elements, but this can cause weakening of the structure in the most crucial parts of the building, thus threatening its stability and integrity. A description and schematic representation of structural details that are critical from the point of view of earthquake resistance can be found in (Azinović *et al*. 2014b). The authors are of the opinion that the suitability of various details and technical solutions used in passive and low-energy buildings located in earthquake-prone areas should be verified from the viewpoint of their earthquake resistance engineering design before they are implemented. Up until now there has been a lack of research dealing with the concept of placing a layer of thermal insulation (TI) below building foundation slabs from the point of view of earthquake resistance.

In general, when flexible layers of TI are inserted between the RC foundation slab and the levelling concrete on the ground (Fig. 1(a)-(b)), the fundamental period of the structure is elongated (T_{TI}>T_{FB}) due to the shear as well as the vertical deformability of the TI layer. Most passive houses are low-rise buildings with short fundamental periods which would be lengthened by the insertion of a TI layer, and thus moved into the resonance part of the Eurocode 8 (CEN 2005a) elastic response spectrum, where the expected top accelerations of the structure could be two or three times greater than in the case of a fixed-base (FB) structural variant. Such an increase might lead to structural damage to the superstructure and contents of the building, and should therefore not be ignored. As a consequence of rocking behaviour due to strong earthquakes, detachment of the structure from the supporting soil or TI layer could occur at one edge, whereas the TI layer at the opposite edge of the foundations would be over-compressed. Lengthening of the structural period would also result in an increase in the top displacements (Fig. 1(b)). However, if the superstructure's fundamental period T_{FB} lies within the range defined by the plateau of constant accelerations, the insertion of a layer of TI beneath the foundation slab might move the structural period into the descending branch (T_{TI}>T_C). Only in this case does the TI layer act as a seismic

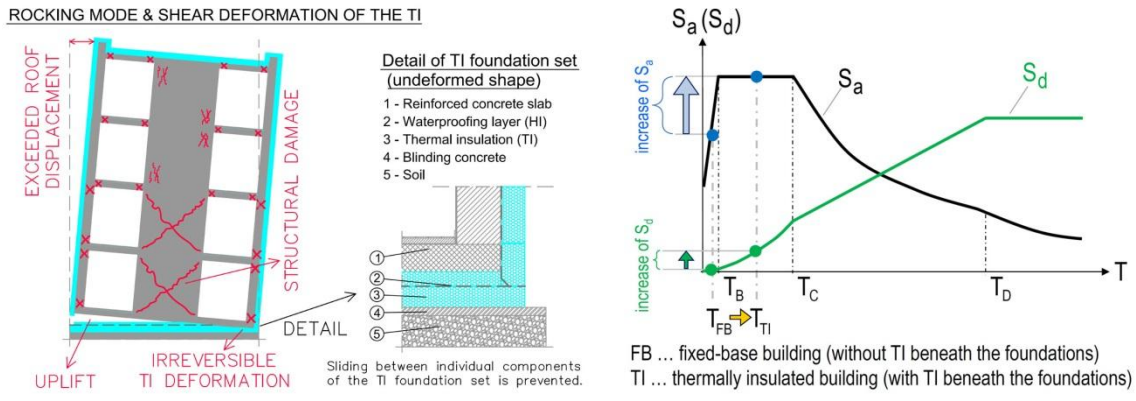

Fig. 1 Building founded on TI layer(s) and its potential seismic response (a) and the spectral roof accelerations (S_a) and displacements (S_d) (b)

base isolation system (Naeim and Kelly 1999, Kilar and Koren 2009, Koren and Kilar 2011, Mahmoud *et al.* 2012, Varnava and Komodromos 2013, Islam *et al.* 2013a, 2013b, Cheraghi and Izadifard 2013, Anagnostopoulos *et al.* 2015), with a reduction in the expected earthquake induced forces.

A short review of research dealing with TI made of extruded polystyrene foam (XPS) has shown that the available studies mostly concentrate on its energy efficiency (Ohara *et al.* 2004, Bunge and Merkel 2011, Vo *et al*. 2011). An investigation into the relationship between the microstructure of XPS foam and its response under compressive stresses has been performed by Sadek and Fouad (2013). It should be noted that the time-dependent behaviour of XPS can substantially affect its structural seismic response. The long-term mechanical properties of XPS have been analysed by Merkel (2004), who showed that these properties are significantly reduced compared to the short-term ones. The modelling of a foundation slab resting on a TI layer is also schematically indicated in the latter reference.

The cyclic behaviour of extruded polystyrene foam (XPS) in compression as well as in shear has been recently experimentally researched and documented by the authors of the current paper (Kilar *et al.* 2014). The results of a preliminary study concerning the seismic response of buildings with an XPS layer beneath the foundation slab have been presented in (Kilar *et al.* 2013, Koren *et al.* 2013). The main assumption of this study was that the upper building was modelled as a rigid block resting on elastic foundations. It was shown that, in general, the seismic safety of passive houses with heights of up to 2 or 3 storeys is not of critical concern. Since the insertion of TI layers beneath the foundations of a building can result in significant changes in the latter's dynamic characteristics, additional attention needs to be paid to the structural seismic response of such buildings during the design phase. The results of an extensive parametric study of the seismic behaviour of buildings founded on deformable TI layers have been presented in (Azinović *et al*. 2014a), where the upper structure was idealized by a single degree of freedom nonlinear system with a stiff foundation slab lying on an XPS layer modelled by a set of vertical and horizontal nonlinear springs. The analysed buildings were assumed to be founded on very stiff soils, so that soil-structure interaction (SSI) effects were not taken into account. It was concluded that amplifications of selected observed response parameters can be expected in the case of stiffer buildings with higher strength ratios. The amplifications, as might be expected, in general increase with the number of storeys, the slenderness of the building, and the seismic weight of the building. On the other hand, in the case of more flexible structures a positive effect due to a reduction in the superstructure ductility demand was detected.

2. The analysed RC structures and deformable base

2.1 Geometry, modelling, and design of the superstructures

The realistic multi-storeyed RC frame (wall) building which is shown in Fig. 2 was used as a test example. The selected building represents a typical simplified passive or low-energy office-building founded on an RC foundation slab. In order to study the different structural variants, buildings with the same floor plan dimensions (*B/L*) but with varied selected parameters were investigated (Table 1). The original variant was a regular, symmetric, 4-storeyed building, with a total mass equal to 971.2 tons (Koren and Kilar 2014). The analysed building variants were assumed not to have an underground basement. The structural 2D models (frames YZ and XZ)

were analysed by means of the computer program SAP2000 (CSI 2011). All the elements of the 2D load bearing structures were modelled by means of frame line elements that were positioned along lines corresponding to the centre of gravity of the actual cross sections. The effective areas which were taken into account in the case of frames YZ and XZ are indicated in Fig. 2. The beams were modelled as frame elements with rigid links at both ends. The RC foundation slab was modelled by means of a frame line element, taking into account uncracked cross sections with 3 different stiffnesses (Table 1), and assuming elastic behaviour. It was divided into a number of sub-elements, all of which had the same length. The frame elements of the foundation slab under the columns/walls were modelled as being rigid in all cases.

In order to estimate the stiffness which results in the most critical response of the TI models compared to the response of the corresponding FB models, the dimensions of the RC cross sections corresponding to the final test structures were selected in the preliminary stage of the study. For this purpose variants of the 4-storeyed YZ frame in which the columns/walls had different heights (h_c) (Table 1) were analysed by performing linear dynamic response spectrum analyses (RSA). The dimensions of the cross sections of the RC beams (b_b/h_b=30/60 cm) were

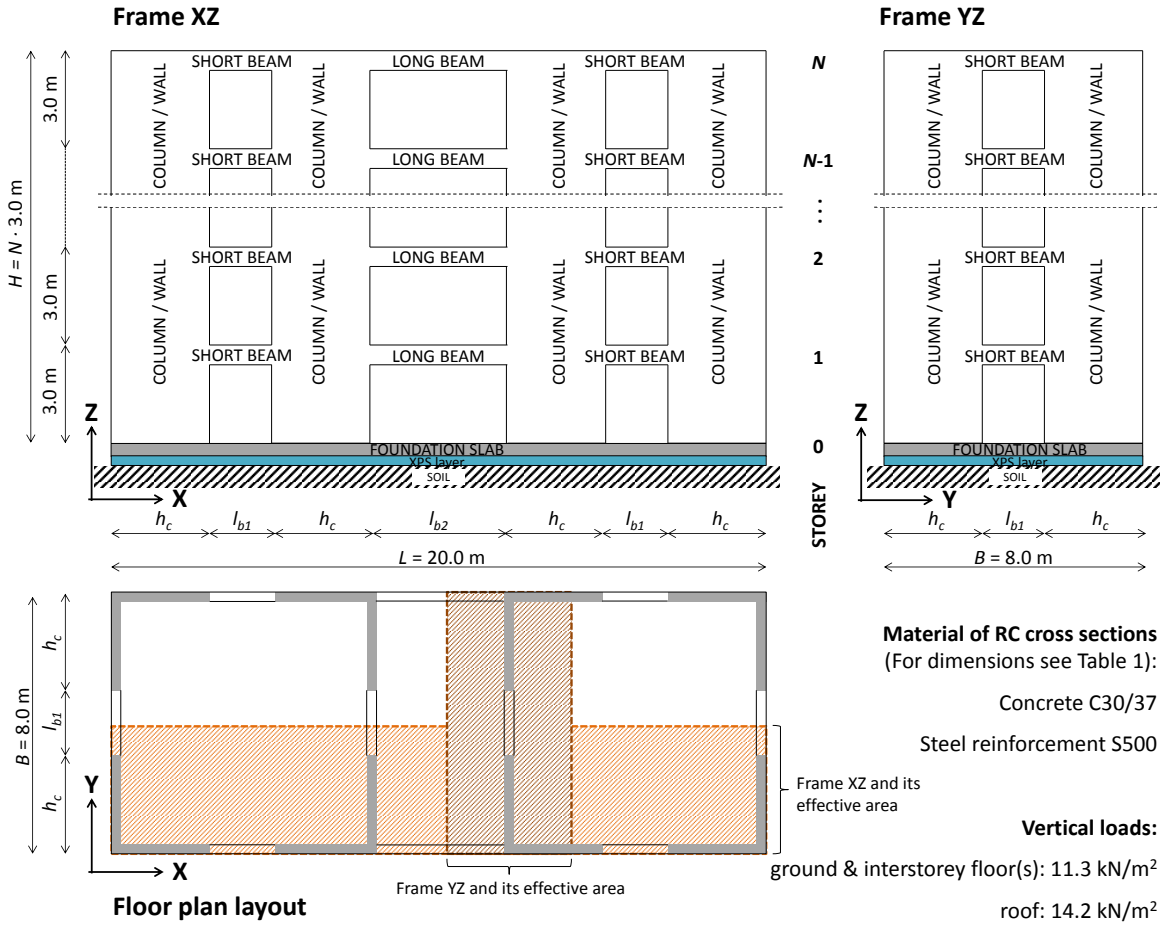

Fig. 2 The investigated office building (BN-TI-soil) and the building's two characteristic frames

equal in all of the investigated cases. The seismic excitation was applied in the horizontal (Y) direction only. The seismic input was defined on the basis of elastic, 5% damping acceleration response spectra that were evaluated for soil type A and a_g=0.25 g, complying with EC8 and assuming corner periods that are in accordance with the corresponding Slovenian National Annex. It should be noted that, in the case of the RSA, only linear elastic stiffnesses were assumed, so that the nonlinear contact springs (modelled to act in compression only) worked in tension as well as in compression, thus preventing any uplift of the foundation slab. The thickness of the RC foundation slab was equal to 30 cm. The TI variant was the same as the FB, the only difference was that an XPS layer (XPS 400) was deemed to be installed between the soil and the foundation slab. Details about the modelling of the soil and the XPS are presented in Section 2.2. The response of frame YZ as related to the dimensions of the columns/walls is presented in Table 2. Comparing the TI/FB amplification factors, it can be seen that the response of the stiffer structures is, in general, more critical than that of the flexible ones. Observing the fundamental periods, the response of the TI models was amplified by a factor of up to 2 compared to that of the FB models, and the amplification factor was even much larger in the case of the observed roof displacements. In the given specific case, when the stiffness of the frame was increased, the fundamental period of the model was shifted towards the left part of the response spectrum plateau - as close as possible to the corner period T_B (see Fig. 1) in order to remain on the plateau also after the period had been elongated due to the insertion of the XPS layer beneath the foundations of the building. For this reason, in the case of the later detailed analyses, the dimensions of the walls were chosen, in the case of both frames (YZ and XZ), to be equal to 30/300 cm.

As can be seen from Table 2, in the case of the finally selected 4-storeyed YZ frame the amplification factor of the fundamental period was 1.75. In the case of the corresponding model of

Table 1 Overview of the varied input parameters, together with their domain and the nomenclature of the building models investigated in the study

		Values/Description
Parameter	Cross-section of the columns/walls (b_c/h_c)	h_c=50 to 350 cm (constant width b_c=30 cm)
	Length of the short beams (l_{b1})	l_{b1}=l_{b1}(h_c)=100 to 350 cm
	Length of the long beams (l_{b2})	l_{b2}=l_{b2}(h_c)=400 to 1100 cm
	Thickness of the RC foundation slab	30 cm, 60 cm, fully rigid slab
	Number of storeys (N)	2, 4, 6
	Soil type	A, C, E & the model without considering SSI
	XPS product	XPS 400, XPS 700 (constant thickness d=24 cm)
	Seismic intensity (a_g)	0.25 g, 0.35 g
Model nomenclature	Ex. 1: BN-FB	N-storeyed Building founded on a Fixed Base (without TI) without taking into account SSI
	Ex. 2: BN-FB-soilA	N-storeyed Building founded on a Fixed Base (without TI) taking into account soil type A
	Ex. 3: BN-TI	N-storeyed Building founded on TI made of XPS 400 without taking into account SSI
	Ex. 4: BN-TI-soilC	N-storeyed Building founded on TI made of XPS 400 taking into account soil type C

Table 2 The effective fundamental periods (T) and max. lateral roof displacements (D_{roof}) of the frame YZ (B4-FB-soilA and B4-TI-soilA) depending on the dimensions of the columns/walls: RSA, a_g=0.25 g

	Cross sectional dimensions (b_c/h_c) of the columns/walls [cm]						
	30/50	30/100	30/150	30/200	30/250	**30/300**	30/350
T_{FB} [sec]	0.835	0.557	0.402	0.301	0.220	**0.160** (63 / 74)*	0.114
T_{TI} [sec]	0.899	0.651	0.515	0.414	0.336	**0.280** (74 / 78)*	0.249
T_{TI}/T_{FB}	1.08	1.17	1.28	1.37	1.53	**1.75**	2.18
$D_{roof,FB}$ [mm]	64.94	44.30	32.19	18.17	9.65	**5.14**	2.60
$D_{roof,TI}$ [mm]	70.14	52.07	41.97	33.67	22.90	**15.79**	12.35
$D_{roof,TI}/D_{roof,FB}$	1.08	1.18	1.30	1.85	2.37	**3.07**	4.75

*the modal participating mass ratios [%] (for the lateral / rocking direction) are given in parentheses

the XZ frame the amplification was smaller (1.48), although the fundamental period (T_{FB}=0.168 sec) was almost the same as in the case of YZ frame. It should be noted that, for both frames, the 1st mode was always a combination of the oscillation in the building's lateral direction and the rocking mode. From the modal participating mass ratios shown in Table 2 (only for the model with the finally selected dimensions of walls) it can be seen that, in the 1st mode of oscillation, the contribution of rocking is larger than that of the oscillation in the lateral direction. It should be noted that this is not so in the case of the squat (i.e., XZ) frame, where in the 1st mode of oscillation the participating mass ratio for the lateral direction was about twice as large as the corresponding ratio for the rocking direction.

For the steel reinforcement of the selected concrete rectangular cross sections of the beams and walls, the minimum reinforcement for the selected ductility class medium (DCM) according to EC8 was adopted (see Fig. 3). Such minimum reinforcement was intentionally selected in order to avoid over-designed RC cross sections. In this way the amplifications determined in later analyses could be contributed mostly to the studied effects of the insertion of XPS layer beneath the foundation slab. The assumed minimum longitudinal reinforcement, as well as the shear reinforcement, proved to be adequate for the design earthquake load (a_g=0.25 g) modelled using the EC8 response spectrum, with an applied behaviour factor of q = 3. The flexural plastic hinges used in the nonlinear static and dynamic analyses were defined based on the reported longitudinal steel reinforcement.

The nonlinear behaviour of the superstructure was modelled using a lumped plasticity model with plastic hinges at both ends of each beam and wall (taking into account the clear lengths of the elements). Two types of plastic hinges were investigated: (i) bending hinges (beams) and (ii) combined axial-bending hinges (walls). It was assumed that the shear capacity of the structural elements was adequate and that shear failures of the structural elements would not occur. At the end of the calculations the adequacy of the shear capacity of the RC beams and walls used in the study has been proven to be sufficient. The flexural plastic hinge lengths were determined according to (Paulay and Priestley 1992) and they were assumed to be constant during the nonlinear response. The moment-rotation envelopes of the plastic hinges were assumed to be tri-linear with a load drop (Fig. 3) and of symmetric shape (i.e., equal for both directions of the loading) for the plastic hinges in all the beams as well as in the wall frame elements. The initial stiffness (corresponding to the elastic part) was assumed to be equal to 0.5EI (cracked cross sections). The rotation at total collapse was arbitrarily assumed to be equal to twice and five times

the maximum rotation of the walls, and of the beams, respectively (Dolšek and Fajfar 2007, Kreslin and Fajfar 2010). In Fig. 3 the selected limit rotations of the characteristic performance levels (IO, LS and CP) are also presented. The characteristic values of the plastic hinges considered in the study are shown in the table in Fig. 3. The maximum moment M_{max} was determined for each element by means of moment-curvature analysis using SAP2000 Section Designer, where the axial forces resulting from the vertical loadings were considered. For the modelling of the material hysteretic behaviour which was considered in the moment-curvature analysis of the RC cross sections the cyclic behaviour based on Takeda rules was assumed for the modelling of the concrete, whereas for the modelling of the steel reinforcement a kinematic hysteretic model was used.

It was recognized that seismic soil-structure interaction (SSI) could have a possible detrimental effect on the behaviour of the superstructure (Mylonakis and Gazetas 2000, Bhattacharya and Dutta 2004, Giarlelis *et al.* 2011, Mahmoud *et al.* 2012, Jarernprasert *et al.* 2012, Moghaddasi *et al.* 2015), so that in most of the investigated cases of the parametric study it was taken into account by analysing the seismic response of the FB as well as TI building models founded on different soil types.

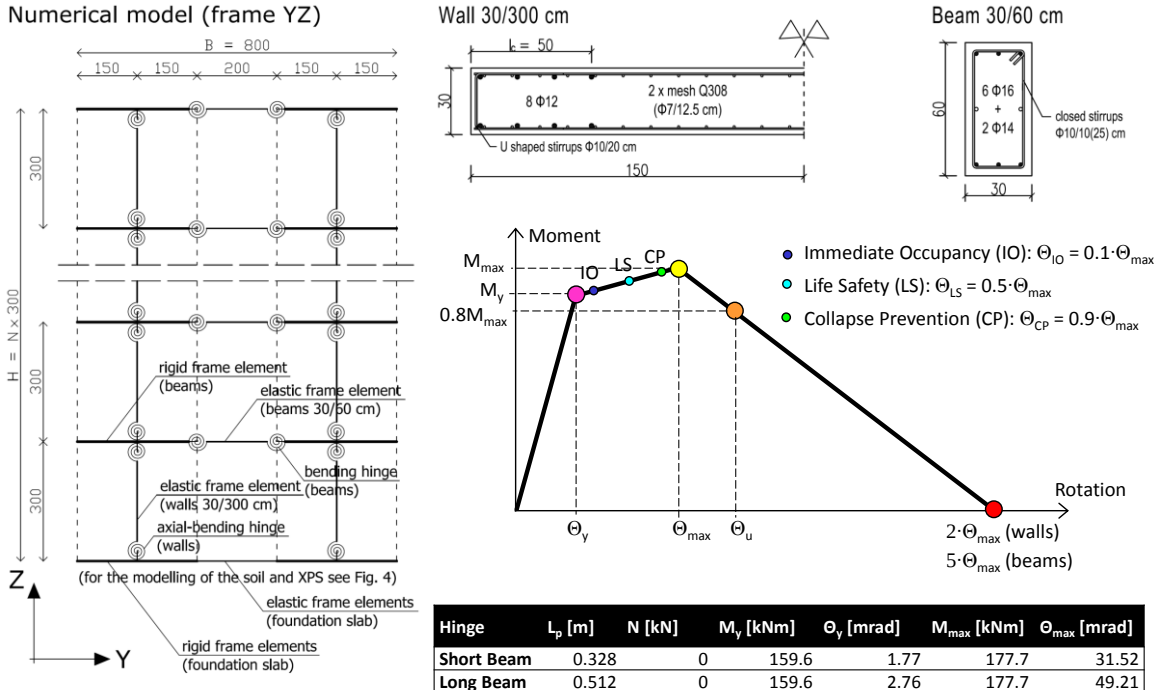

Hinge	L_p [m]	N [kN]	M_y [kNm]	Θ_y [mrad]	M_{max} [kNm]	Θ_{max} [mrad]
Short Beam	0.328	0	159.6	1.77	177.7	31.52
Long Beam	0.512	0	159.6	2.76	177.7	49.21
		1 500	218.2	0.10	724.6	12.70
		0	1 816.2	0.36	2 702.0	7.49
		-2 000	4 161.5	0.41	5 121.5	3.59
Wall	0.372	-6 000	8 146.0	0.50	9 110.9	1.68
		-10 000	11 287.6	0.58	11 656.9	1.08
		-14 000	13 023.8	0.68	12 644.9	0.80
		-19 000	12 494.5	0.51	11 644.4	0.60

Fig. 3 Numerical model, details of the steel reinforcement of the RC elements and the characteristics of the plastic hinges considered in the study

2.2 Characteristics and mathematical modelling of the soil and XPS

In the parametric study four different soil conditions were analysed (Table 1 and Fig. 4) - two models (with stiff restraints) where soil stiffness as well as uplift was excluded (models: BN-FB and BN-TI) and three models that were deemed to be constructed on real soil types (A, C, and E according to EC8 - models: BN-FB-soil type and BN-TI-soil type). A constant value of ρ=2000 kg/m^3 was assumed for the soil density in all the investigated soil types. The shear-wave (v_s) velocities were selected according to EC8: v_s=2500 m/s, 300 m/s, and 100 m/s for soil types A, C and E, respectively. For calculations of the longitudinal- (primary-) wave (v_p) velocity, the relationship v_p=2.5·v_s was adopted. The soil shear modulus (G) and Poisson's ratio (ν) were calculated from the following expressions (Mahmoud *et al.* 2012, Sykora 1987)

$$G = \rho \cdot v_s^2 \qquad \nu = \frac{0.5 \cdot (v_p / v_s)^2 - 1}{(v_p / v_s)^2 - 1} \tag{1}$$

For the modelling of the soil the Winkler foundation model was applied. The behaviour of the soil in shear was modelled by linear elastic springs. Since, in practice, no tensile resistance is provided by the soil-structure contact, so that the foundation could partially uplift from the soil surface (Apostolou *et al*. 2007, Gelagoti *et al*. 2012, Ghannad and Jafarieh 2014, Makris 2014), the behaviour of the soil in compression was modelled by nonlinear contact springs. This approach differs to some extent from that used in some previous studies of buildings founded on an elastic half-space modelled by swaying and rocking spring-dashpots and neglecting uplift (Wolf 1997, Wu and Lee 2002, Mahmoud *et al.* 2012). The soil springs were modelled in the SAP2000 software as one-joint link/support elements of the Multi-Linear Plastic - Kinematic type, which are available in the program with stiffnesses that correspond to the effective area that is equal to the product of the length of the finite elements equal to 0.50 m and the considered effective width (Fig. 4). In the case of studied building plan the dynamic stiffness coefficients (Gazetas 1991) equal to 1.0 were taken into account for the vertical (k_Z,) as well as for the longitudinal (k_X) directions. For the lateral direction (k_Y) its value was taken equal to 1.25. The damping of the soil springs in both of the active directions (i.e., axial and shear) was assumed to be equal to zero (Mahmoud *et al.* 2012). The soil stiffnesses considered in the study are shown in Table 3.

Table 3 The soil stiffnesses for the studied building floor plan (L_x/L_y=20/8 m)

	Soil A	Soil C	Soil E
k_Z [kN/m]	632 000 000	9 100 000	1 000 000
k_X [kN/m]	450 000 000	6 500 000	700 000
k_Y [kN/m]	617 000 000	8 900 000	1 000 000

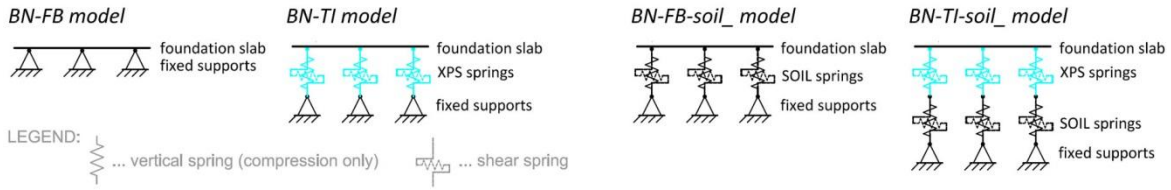

Fig. 4 Schematic presentation of the foundation modelling variants considered in the study

When analysing the behaviour of the XPS material (in compression as well as in shear), the stress-strain curves which were obtained experimentally (Kilar *et al.* 2014) were idealized and applied. XPS boards having two different nominal compressive strengths (400 and 700 kPa) were used in the analysis. The axial cyclic behaviour of the XPS was modelled by means of a kinematic hysteretic model, whereas a Pivot hysteresis loop was assumed for the cyclic behaviour in shear, taking into account the following parameters: $\alpha_1=\alpha_2=1.0$, $\beta_1=\beta_2=0.25$ and $\eta=0$. The effective stiffnesses were assumed to be equal to the initial stiffness of the material. The rotational degree of freedom of the XPS spring was fixed.

The thermally insulated (TI) models were derived from the fixed-base (FB) models by adding XPS two-joint springs modelled in series with one-joint soil springs below (Fig. 4). The length of the XPS springs was equal to the total thickness of the XPS layer (24 cm). In the analysis it was assumed that sliding at the contact between the different layers of the TI foundation set (Fig. 1) is prevented. Apart from the TI and FB models which included SSI effects, other corresponding models in which the soil was not modelled were also taken into account (Fig. 4).

2.3 Loading for the nonlinear seismic analyses

The seismic analyses of the investigated frame systems were carried out by means of nonlinear static analysis and nonlinear dynamic (time-history) response analysis. The vertical loads which corresponded to the seismic limit state defined in EC8 were assumed as the initial loads in all the seismic analyses (Fig. 2), where uni-directional (horizontal) seismic excitation was applied.

Nonlinear static (pushover) analyses were performed in order to assess the global seismic response of the considered building models without calculating the seismic demand values. In these analyses the lateral load distribution shape corresponded to the mass proportional to the displacement of the 1st mode of the structure's eigen oscillation, with initial stiffness considered.

In the nonlinear dynamic analyses (NLDA), two groups of 7 different ground motions with two different PGA levels (a_g=0.25 g and a_g=0.35 g) were applied. The first group ("group 1") consisted of an ensemble of seven EC8 spectrum-compatible artificial accelerograms generated by the program SYNTH (Naumoski 1998). As a target spectrum, the EC8 elastic spectrum for the selected soil type (A, C or E), scaled to a peak ground acceleration of a_g=0.25 g for a 5% damping ratio, was used. The acceleration spectra of the generated accelerograms are presented, for soil type A, in Fig. 5. The same group of ground motion records was also used in the authors' previous studies (Kilar and Koren 2009, Koren and Kilar 2011). In order to obtain a more realistic seismic response, a group of 7 real earthquake records was also applied ("group 2"). The selection was made by means of REXEL software (Iervolino *et al.* 2010), taking into account the condition that the records match the EC8 elastic spectrum for soil type A and a_g=0.25 g. In order to be able to find suitable one-component record sets, a spectrum compatibility tolerance between 10% (lower) and 15% (upper) in the range of the period of interest [0-0.5 s] was specified. The selection of the periods of interest was performed in accordance with the obtained fundamental periods of the analysed models (see Table 2). Additionally, a range of magnitudes equal to [5.0-7.5] was applied, whereas values between an upper limit (50 km) and a lower limit (20 km) were selected to define the range of distances. The acceleration spectra of the used accelerograms from the European Strong-Motion Data (Ambraseys *et al.* 2002) provided by REXEL are shown in Fig. 5. In the dynamic analyses, the damping matrix was considered to be proportional to the mass and to the initial stiffness matrices. 5% damping was assumed in the first and second modes of vibration. The damping of the soil, as well as of the XPS layer, was assumed to be negligible.

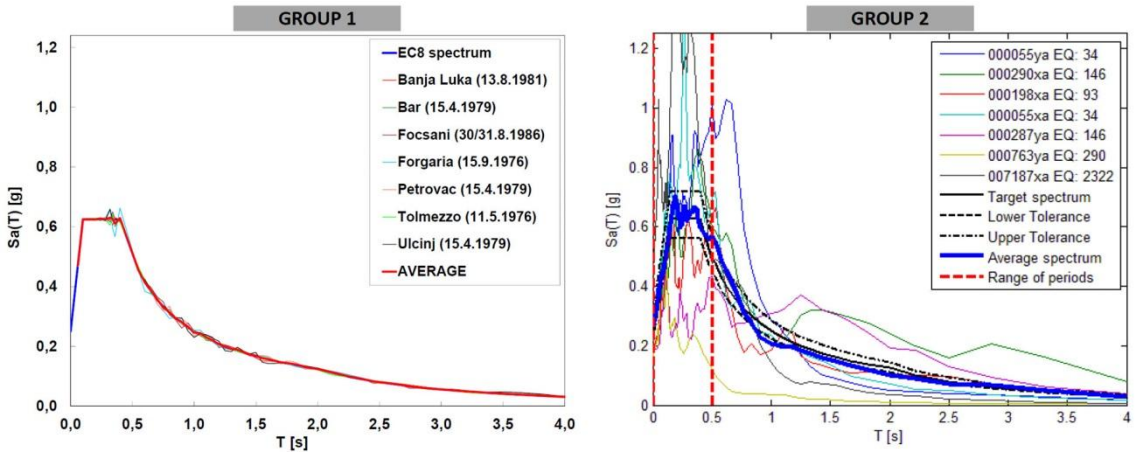

Fig. 5 The response spectra of the used generated (group 1) and real (group 2) accelerograms

3. Evaluation of the building's seismic response and discussion of the results

3.1 The observed performance parameters

The structural response of the analysed systems was investigated with respect to the following performance parameters: (i) the building's lateral roof displacements, (ii) the XPS edge compressive and shear strains, (iii) the horizontal accelerations of the superstructure measured at different storey levels of the building, (iv) the plastic hinge patterns and/or interstorey drifts of the superstructure, (v) the part of the foundation in compression, and (vi) the vertical displacements (i.e., deformed shape) of the foundation slab (possible uplift).

Most of the performance parameters are presented in terms of the maximum obtained values calculated by nonlinear dynamic analysis (NLDA). For the selected performance parameters the maximum structural response and/or the time-history in the case of a selected accelerogram are also presented. The global seismic response of the considered building models is shown for the selected performance parameters also in terms of the obtained pushover curves. An extensive presentation of the results obtained in the pushover analyses has been given in (Koren and Kilar 2014).

3.2 The response of the original test structure

The seismic response of the original structure (i.e., the 4-storeyed YZ and XZ frames, a_g=0.25 g, soil A, 30 cm thick foundation slab, XPS 400) is presented in Figs. 6-8, and to some extent in some of the figures and tables in the following sections when investigating the effects of selected input parameters. The lateral roof displacements and maximum edge compressive deformations of the XPS layer are shown in Fig. 6, where the results are presented as envelope values for each applied seismic ground motion record. As can be seen from Fig. 6, the structural response corresponding to the group 1 of accelerograms is, with some smaller deviations, similar to that corresponding to group 2. Somewhat larger differences can be seen in the case of the building's lateral displacements. Comparing the calculated maximum compressive deformations in the XPS

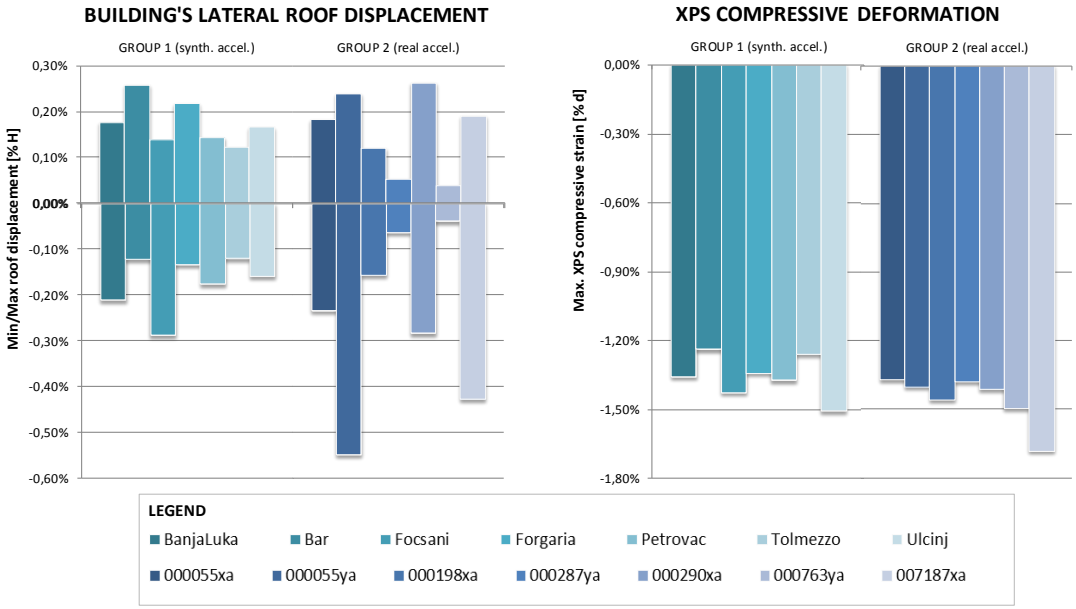

Fig. 6 The response of the B4-TI-soil A (frame YZ) in relation to the applied seismic ground motion records: a_g=0.25 g, 30 cm thick foundation slab

layer, a very good agreement between the results obtained when applying both groups of accelerograms can be noted. It can also be seen that, in most cases (with two exceptions in the case of real earthquake records), the calculated displacements do not exceed the limit values which were selected to be equal to 0.33% of the building's total height (*H*) (CEN 2004) and 2.1% of the thickness of the TI (XPS) layer (*d*) for the lateral roof displacement and the XPS compressive deformation, respectively. Similarly, the maximum obtained shear deformation (γ_{XPS}) in the XPS layer did not exceed its yield limit (2.9% *d*) - the maximum obtained values varied between 0.5% and 0.75% of the thickness of the XPS layer (*d*). Similar observations were made when analysing the response of the XZ frame.

The typical obtained damage patterns of the FB and TI frames YZ and XZ are presented in Fig. 7, together with the absolute maximum accelerations measured at different building storey levels. The damage patterns show the performance levels of the superstructure (measured with reference to the calculated rotations in the generated plastic hinges - see Fig. 3). It can be seen that the obtained damage states are higher in the case of buildings built on a layer of XPS. Moreover, in the case of the analysed TI frame structures partial collapse mechanisms were formed - see the generated plastic hinges in the walls which were not recorded in the case of the analysed FB frames. However, these performance levels are only slightly beyond the defined yield limit. Comparing the response of the TI and FB models in terms of the average absolute maximum accelerations, it was observed that the TI/FB amplifications have significant values (~1.6 for the YZ frame and ~2.7 for the XZ frame) in the case of accelerations measured at the ground floor level. On the other hand when the TI and FB accelerations at the roof level are compared, the amplifications were small. This means that in the analysed model the accelerations of the ground floor are significantly larger in the case of buildings built on a layer of XPS. Comparing the soil (input) accelerations and the accelerations transferred to the top of the ground floor slab, it is clear

that significant amplifications (~1.6 for the YZ frame and ~2.5 for the XZ frame) occur in the case of the TI models, whereas in the case of the FB models these amplifications are practically negligible ($a_{ground\ floor} \approx a_{soil}$). Here it should be mentioned that such a response is quite different to that of structures which are base-isolated by means of seismic isolation devices (e.g., rubber bearings and friction-pendulum isolators), where the accelerations at the top of the ground floor slab are significantly reduced due to the considerable elongation of the fundamental period of vibration (Naeim and Kelly 1999, Kilar and Koren 2009, Koren and Kilar 2011, Mahmoud *et al.* 2012, Varnava and Komodromos 2013, Islam *et al.* 2013a, 2013b, Cheraghi and Izadifard 2013, Anagnostopoulos *et al.* 2015). Additionally, in the case of structures which are base-isolated by means of seismic isolation devices the amplifications of accelerations along the building's height are, in general, very small, which was to some extent observed in the case, described in this paper, of a structure isolated with an XPS layer beneath the foundation slab. As can be seen from Fig. 7, the amplifications of the accelerations along the TI building's height ($a_{roof}/a_{g.floor}$) were around 1.4 and 1.3 for the YZ and XZ frames, respectively. On the other hand, in the case of the FB models these amplifications were considerably larger (~2.3 for the YZ frame, and ~3.2 for the XZ frame). Similar findings in connection with the obtained damage patterns and the absolute maximum accelerations were made also in the case when the synthesized ground motions (group 1) were applied (Koren and Kilar 2014).

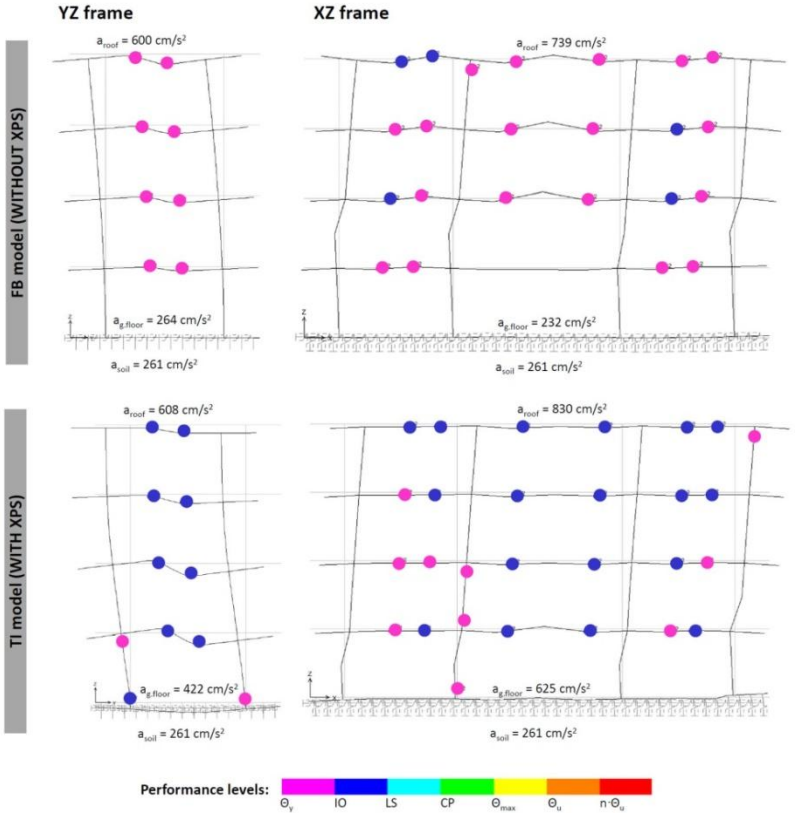

Fig. 7 Typical damage patterns and the average absolute maximum accelerations of the B4-FB-soilA and B4-TI-soilA frames subjected to group 2 of accel.: a_g = 0.25 g, 30 cm thick foundation slab

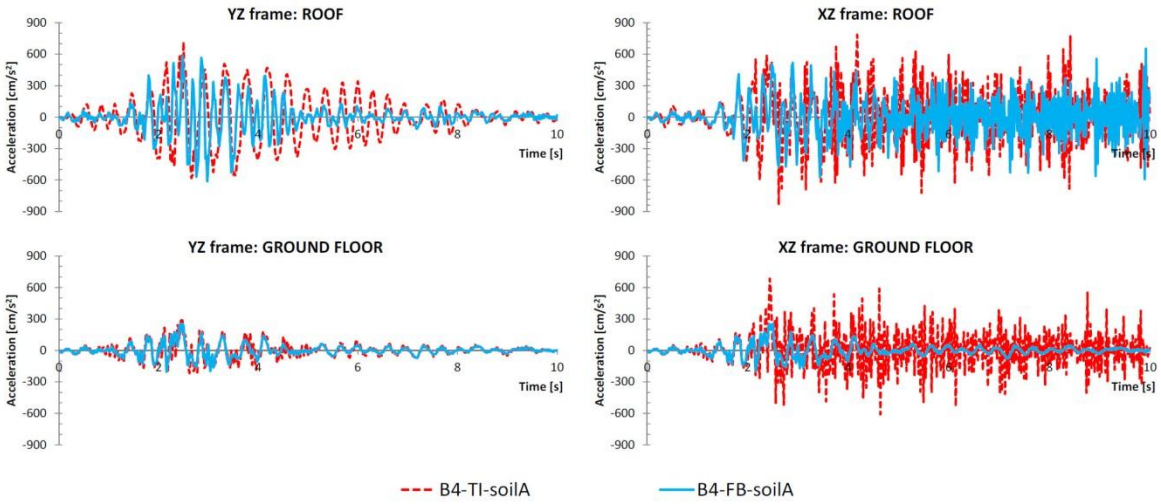

Fig. 8 Absolute accelerations of the B4-FB-soilA and B4-TI-soilA frames when subjected to the synthesized accel. Banja Luka: a_g=0.25 g, 30 cm thick foundation slab

The time-history diagrams of the absolute accelerations at different storey levels when subjected to a selected synthesized accelerogram (Banja Luka) are shown in Fig. 8. The time-history of the soil (input) accelerations, which for the sake of brevity is not shown, is almost equal to the accelerations measured at ground floor level in the case of the FB models. The presented time-histories mostly confirm the above-mentioned findings about the amplifications of the accelerations along the building's height and about the differences between the responses of the FB and TI models. It should be noted that the time-histories differ considerably with respect to the observed frequencies.

3.3 The effect of the soil type

As can be seen from the results presented in Figs. 9-11 and Table 4, the structural response is considerably affected by the soil type. The obtained pushover curves for the FB and TI frames YZ on different soil types are presented in Fig. 9, whereas the corresponding results of the NLDA are shown in Table 4 and Figs. 10-11. From the initial slopes of the pushover curves shown in Fig. 9 it can be seen that the response of the thermally insulated (TI) model on firm soil type (i.e., B4-TI-soilA) is equal to the response of the model in which soil stiffness is not included (B4-TI). Such an assumption was made in (Azinović *et al.* 2014a, b). It should be noticed, that the corresponding pushover curves in Fig. 9 coincide. Since soil type A actually represents very firm soil conditions, in the analysed case a comparison of the response of the structure with/without modelling the soil mainly shows the difference between the model with/without consideration of the uplift of the foundation slab. Comparing the response of the FB and TI models on different soils, it can be seen that the TI models are more flexible and that the amplifications are more pronounced in the case when the models are founded on firm soils. In the case of soil E, the effect of poor soil conditions prevails, so that the response of the FB and TI models is almost the same. An additional finding which was made from the pushover analysis of frame YZ was that, in all of the investigated models, at large displacements deep nonlinear behaviour of the soil or the XPS layer occurred,

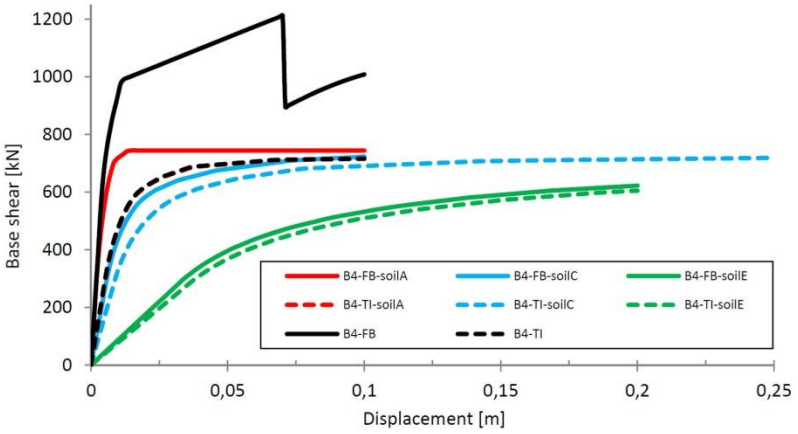

Fig. 9 The obtained pushover curves under different soil conditions: the 4-storeyed FB and TI frame YZ, 30 cm thick foundation slab

whereas a plastic mechanism did not form in the upper frames. The only exception was that of the FB variant of the YZ frame without modelled soil stiffness (see Fig. 9 - the very clear jump in the obtained pushover curve at large displacements). In all the other investigated cases the upper structure behaves like a (semi-)rigid box on a soft layer, where the overall response is governed by the stiffness of the bottom layer. In extreme situations the global stability of the structure (i.e., with possible overturning of the building) was called into question.

The results of the NLDA which are presented in Table 4 confirm that the largest TI/FB amplifications (which for the observed parameters T and D_{roof} can be calculated from the quoted values) were achieved in the case when the building was founded on firm soil. However, based on the absolute values of the quantities under investigation it can be seen that the largest overall response was obtained in the case of poor soil conditions (e.g., in the case of the TI model and soil type E the fundamental period was around 2.7-times larger than in the case of soil A, the corresponding roof displacement (D_{roof}) was more than 3.5-times larger, the XPS shear demand ratio (f) and the shear strain (γ_{XPS}) 1.25-times and 1.15-times larger, respectively, and the maximum XPS compressive strain (ε_{XPS}) 1.05-times larger). Such differences in an absolute response are a consequence of the prolonged fundamental period due to a deformable base (the rocking mode of oscillation), and do not necessarily result in the superstructure having larger ductility demands. In the analysed cases the largest ductility demands were obtained in the case of better soil conditions (soil A and C) - see Fig. 10. Comparing the obtained average absolute maximum accelerations it can be seen that the values are similar for all soil conditions except in the case of the frame on soil type E. Additionally, it was only in this case that a deamplification in the absolute accelerations was observed along the whole of the building's height. The obtained values of the accelerations of frame YZ on soil A when subjected to group 1 of accelerograms were comparable to those obtained when group 2 of accelerograms was applied (see Fig. 7).

In the analysed case analysis of the obtained compressive (ε_{XPS}) and shear (γ_{XPS}) strains and stresses in the XPS (Table 4) revealed that they did not reach their yield limits (the XPS material remained within its elastic range: ε_{XPS}<2.1% d and γ_{XPS}<2.9% d). Observing the shear ratio $f=Q/W$ (where Q is the maximum seismic base shear force induced during earthquake excitation and W is the calculated total seismic weight of the analysed model) which defines the seismic demand for

the friction force between the RC foundation slab and the XPS layer or the friction force demand between the different layers of the XPS foundation set (Azinović *et al.* 2014a), it can be seen that the obtained values are between 0.36 (the models without consideration of SSI) and 0.46 (in the case of soil E). In order to prevent possible uncontrolled horizontal sliding of a building, an appropriate foundation set with sufficient friction capacity has to be used. It should be noted that the application of a foundation set detail where a layer of waterproofing HI material is inserted between the XPS boards (providing a friction capacity equal to 0.27 (Kilar *et al.* 2014)) would, in the analysed case, not be an adequate solution.

Comparing the obtained storey drifts (Fig. 11) which are presented as the average of the maximum and minimum obtained values, it can be seen that in the case of soft (type E) soils the differences between the FB and TI models are negligible. It should be noted that the height-wise distribution of storey drifts depends strongly on the soil conditions (a constant distribution in the case of soil type E vs. a trapezoidal distribution in the case of the model without consideration of SSI). The largest storey drifts were obtained in the case of structures founded on soft soil. However, even these drifts did not exceed the storey drift limit (1.0%) according to EC8 (Part 4.4.3.2) for buildings that have non-structural elements made of brittle materials attached to the structure, and taking into account a reduction factor (considering a lower return period) equal to 0.5.

Table 4 Effect of soil type: the average response of the frame YZ: group 1 of accel. (a_g=0.25 g), 30 cm thick foundation slab

	B4-FB	B4-FB-soilA	B4-FB-soilC	B4-FB-soilE	B4-TI	B4-TI-soilA	B4-TI-soilC	B4-TI-soilE
T [sec]	0.156	0.160	0.285	0.712	0.279	0.280	0.365	0.760
D_{roof} [mm]	11.2	11.3	29.1	73.1	23.5	20.9	47.6	75.7
ε_{XPS} [% d]	/	/	/	/	-1.37	1.36	-1.44	-1.44
γ_{XPS} [% d]	/	/	/	/	0.57	0.56	0.61	0.64
f	/	/	/	/	0.36	0.37	0.40	0.46

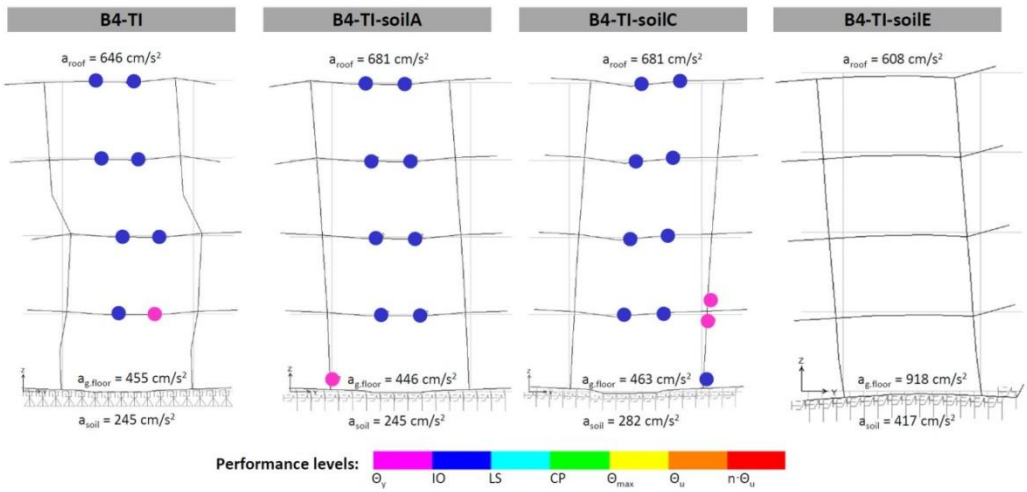

Fig. 10 Effect of soil type: the typical damage patterns and the average absolute maximum accelerations of the frame YZ: group 1 of accel. (a_g=0.25 g), 30 cm thick foundation slab

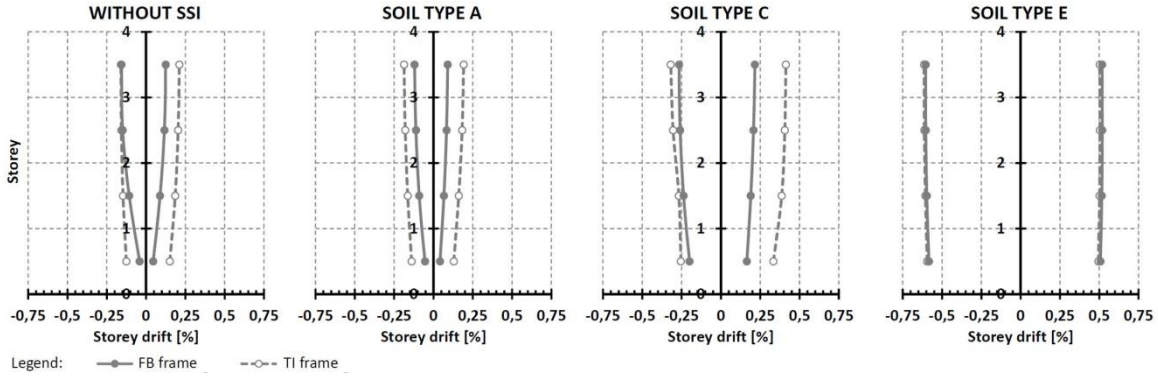

Fig. 11 Effect of soil type: the 4-storeyed frame YZ, group 1 of accel. (a_g = 0.25 g), XPS 400, 30 cm thick foundation slab

3.4 The effect of the foundation slab stiffness

In the authors' previous work (Koren and Kilar 2014) the stiffness of the foundation slab was evaluated as being an important parameter which affects the overall response of the structure, especially when the response of the multi-bay frame (frame XZ) was analysed. If the foundation slab is fully rigid, the distribution of contact compressive stresses in the soil or in the XPS layer is linear (triangular - if the level of the stresses is lower than the soil or XPS yield limit), whereas in the case of a flexible foundation slab the contact stresses become discretely distributed (Fig. 12).

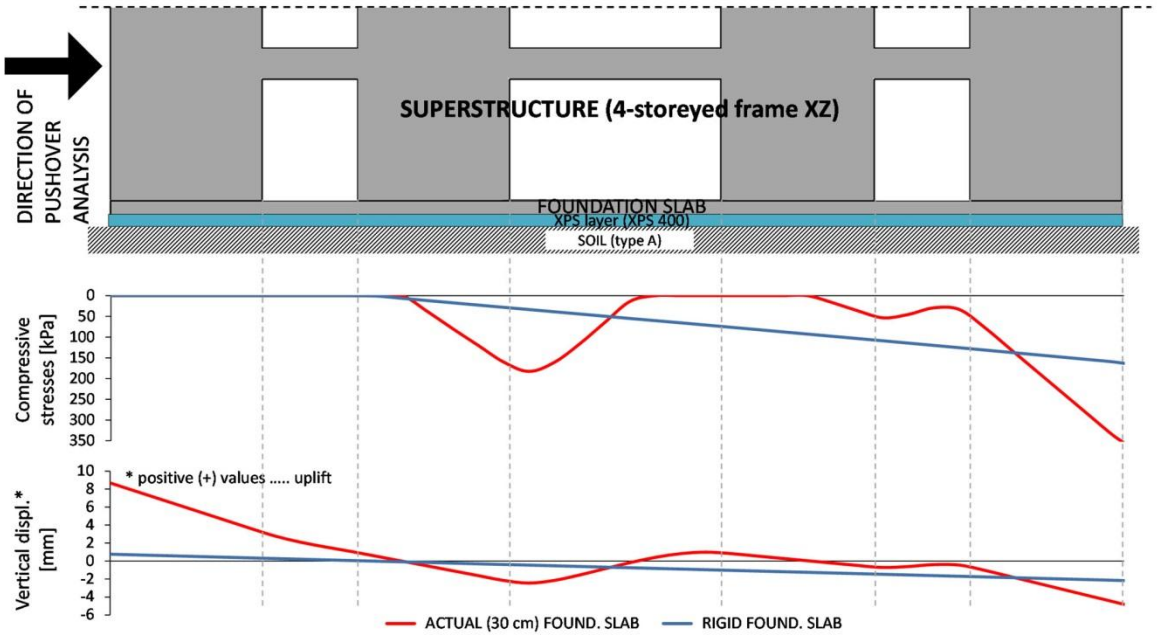

Fig. 12 Effect of foundation slab stiffness - the obtained contact compressive stresses and vertical displacements of the foundation slab (pushover, $D_{x,roof}$ =2.7 cm)

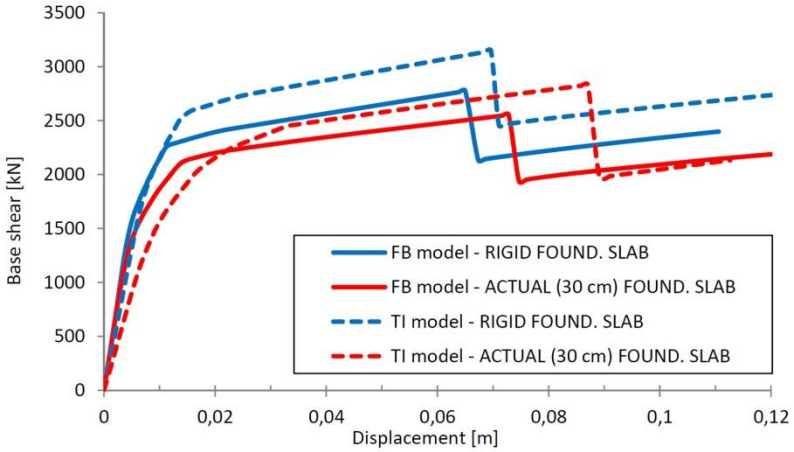

Fig. 13 The obtained pushover curves in relation to the foundation slab stiffness: the 4-storeyed FB and TI frame XZ on soil A

The models on more flexible foundation slabs are more susceptible to larger compressive stresses in the soil or in the XPS layer at one edge of the foundation slab and/or uplifts on the opposite edge. In our analysed case the maximum edge compressive stresses under the actual (30 cm thick) foundation slab are approximately twice the size of the stresses which occur in the case of foundation on a fully rigid slab. Due to the elastic behaviour of the XPS the same conclusion can be made when observing the edge vertical displacements of the foundation slab in a downwards direction. Moreover, when observing the maximum positive values of the vertical displacements (i.e., the occurrence of uplift), the differences between the deformations of the actual and rigid foundation slab are considerably larger. For this reason when attempting an accurate seismic analysis of a building the actual stiffness of the foundation slab should be taken into consideration.

Comparing the pushover curves corresponding to frame XZ on a fully rigid and an actual (30 cm thick) foundation slab (Fig. 13), it can be seen that the differences between the FB and TI models are larger in the case of a flexible foundation slab, whereas in the case of a rigid foundation slab the corresponding pushover curves coincide (see their initial part). Also, in the case of the displacements of the superstructure, larger TI/FB amplifications were observed when the models were founded on an actual foundation slab. Additionally, it should be noted that in the final stage of the pushover analysis the frame XZ reached a completely plastic mechanism, which in general was not observed when analysing the YZ frame (see also Fig. 9). A detailed comparison of the response of the XZ frames with a fully rigid and an actual foundation slab subjected to group 1 of accelerograms can be found in (Koren and Kilar 2014).

3.5 The effect of the XPS class

In order to investigate the effects of the XPS class on the response of the TI models, both frames (XZ and YZ) were analysed on TI boards made of XPS 400 and XPS 700. In both cases the XPS layer had a thickness of d=24 cm. For this purpose only the models with an actual (30 cm thick) foundation slab lying on soil type A were taken into consideration. In this particular case,

the structural overall response was only slightly affected by the class of the XPS boards placed beneath the foundation slab. The fundamental periods of the frames on stiffer XPS class boards (XPS 700) were up to 10% shorter than those of the frames on softer XPS. Similarly, the differences between the obtained damage patterns of the frames on XPS 400 and 700 were negligible. As can be seen from Fig. 14, the response was, in general, decreased if XPS 700 was applied. For example, the lateral roof displacement of the XZ frame on XPS 700 had a value which was equal to ~70% of the corresponding displacement in the case of applying XPS 400. Similar findings were made also for the base displacements in the lateral and vertical direction. For the latter (D_z), it should be mentioned that its negative value indicates compressive deformation of the XPS layer, together with the deformation of the soil below, whereas its positive value indicates the amount of uplift. In our particular case (considering firm soil A) the contribution of the soil to the total compressive deformation was relatively small (~10%). Thus, around 90% of the presented D_z occurred in the XPS layer. From the obtained vertical displacement values it can be concluded that the XPS yield compressive deformation values (2.1 (2.7) % of the thickness (d) of the XPS 400 (700) layer) were never reached. Similarly, according to the yield shear limit of the XPS the lateral base displacements of the ground floor slab were not of critical concern. Due to the SSI modelling in the FB models, only very small vertical base displacements were observed, whereas the lateral base displacements were negligible. Additionally, from the response of frames YZ and XZ shown in Fig. 14 an important general difference can be seen, i.e. that the YZ frame is (due to its height-to-width ratio) much more susceptible to edge uplifts and larger compressive deformations of the ground soil and XPS layer. Moreover, in the case of the YZ frame the obtained uplift D_z displacements are even larger than their compressive values, which was not observed in the case of the XZ frame.

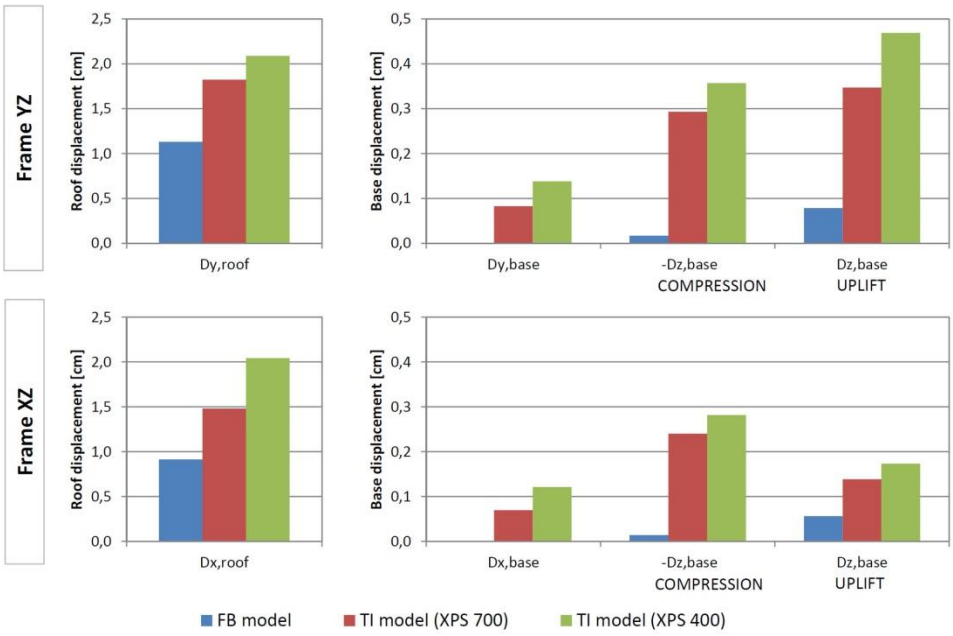

Fig. 14 Effect of the XPS class: average displacements of the B4-TI-soilA frames, group 1 of accel. (a_g= 0.25 g), 30 cm thick foundation slab

3.6 The effect of building height (i.e., the number of storeys)

From the point of view of load bearing capacity with respect to vertical loads only, the use of a relatively soft TI layer beneath the foundations is limited by the building's weight, which is related to the used building materials, the actual live load, and the number of storeys. Taking into account the horizontal dynamic earthquake loads, these parameters take on greater importance. For this purpose in this study the effect of the number of storeys was analysed on the YZ frame with a RC foundation slab of actual stiffness (30 cm thick) on soil type A and XPS 400 subjected to group 1 of accelerograms (a_g=0.25 g). Two and six storeyed models were analysed, as well as the 4-storeyed model, taking into account the same RC cross-sectional dimensions and steel reinforcement as in the case of the 4-storeyed frame.

As can be seen from Fig. 15, the response TI/FB amplifications (for the fundamental period and the lateral roof displacement) decrease when the number of storeys is increased. In the case of the analysed 6-storeyed model, even a slight de-amplification effect was observed for the lateral roof displacement. However, in the analysed cases, the absolute values of the displacements were not of critical concern. Observing the response quantities of the XPS layer (see the TI models in Fig. 15) it can be seen that the maximum compressive strains (ε_{XPS}) in the XPS were achieved in the case of 6-storeyed frame. However, the compressive deformations did not reach the XPS 400 yield deformation value (2.1% *d*). Similar findings can also be made with respect to the shear deformations (γ_{XPS}) of the used XPS, although the differences between the obtained values for the analysed frames with different numbers of storeys were not so pronounced. Observing the shear ratio $f=Q/W$, which defines the seismic friction demand coefficient for the applied TI foundation set, it can be seen that, from this point of view, the low-rise buildings are critical. The maximum obtained value slightly exceeds the friction capacity (~0.5) of the contact between the levelling concrete and the XPS (Kilar *et al.* 2014). It should be noted that the herein reported maximum standard deviations of the response quantities were always obtained in the case of the 6-storeyed frame, and assumed values of up to 90%.

Comparing the obtained typical damage patterns of the 2-, 4- and 6-storeyed YZ frames (Fig. 15) it should be noted that the 2-storeyed frame did not suffer any damage neither in the case of FB nor in the case of the TI structural variant. For the higher buildings the TI models in general reached more critical damage patterns than the FB models. In the case of the 6-storeyed model the obtained damage patterns in the FB and TI models are comparable. Similar conclusions can be made also concerning storey drifts.

In order to obtain a more detailed insight into the behaviour at the foundation level, a time-history response of the B6-TI-soilA model subjected to a selected accelerogram is presented in Fig. 16, where (at the top) the time-history of the vertical base reaction has been plotted. It can be seen that it oscillates around a value of 2632 kN, which is equal to the total weight (W) of the analysed frame at the seismic limit state. Checking the axial forces in all the discretely applied XPS springs, the time-history of the percentage of the foundation (C_p) in contact with the TI can be plotted. Such a presentation is made in the bottom part of Fig. 16 in order to identify how likely it was that uplift of the foundation slab would occur, this being a probable response in the case of slender buildings (with a larger height-to-width ratio). It can be seen that the minimum C_p occurred at t=2.86 s, and assumed a value equal to 43.8% of the dimension B=8 m. It should be noted that, in the case of structures reaching a C_p of 50% or less, EC7 (CEN 2005b) prescribes the application of special precautions in the design of the foundations.

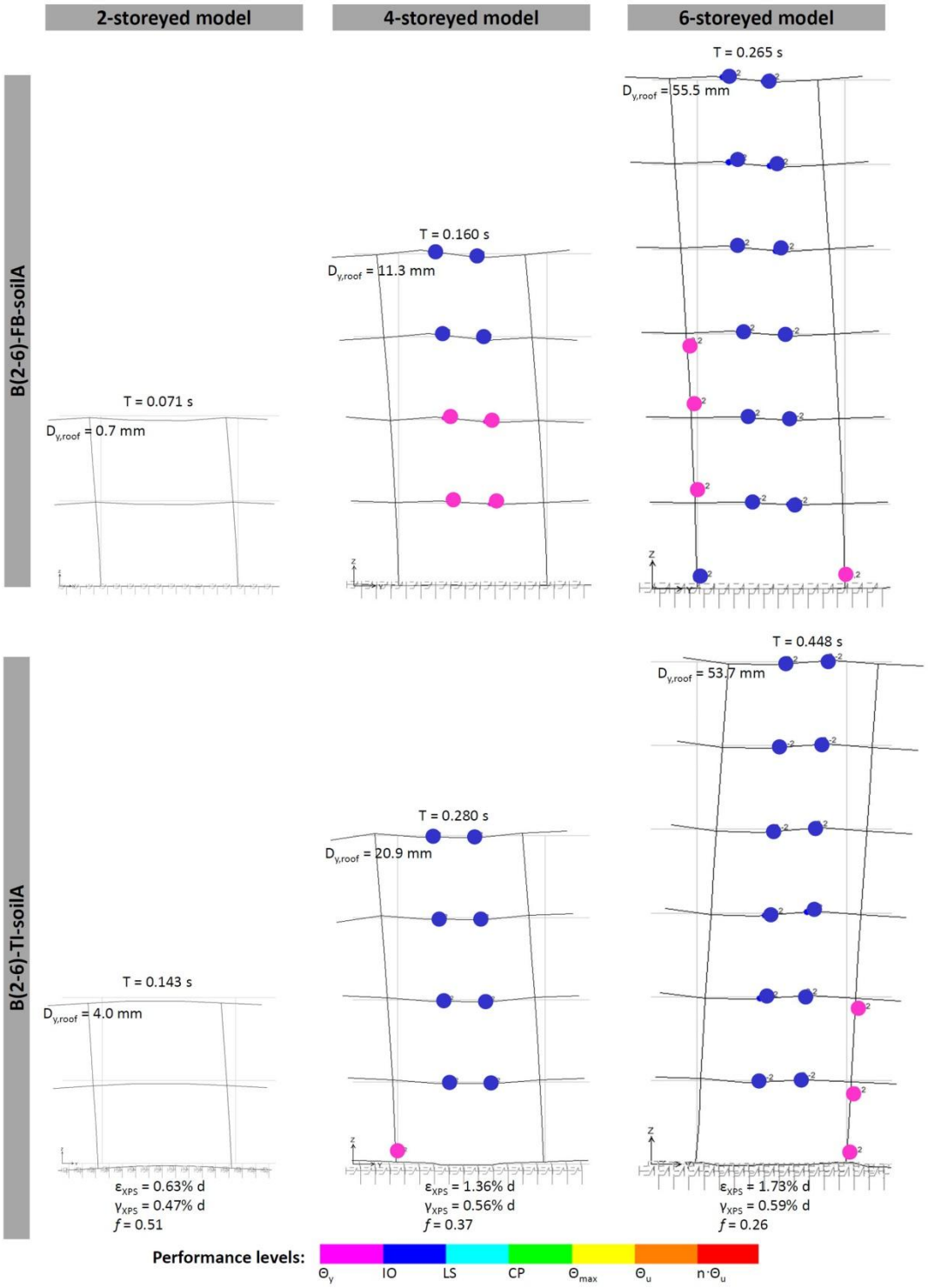

Fig. 15 Effect of the number of storeys: the typical damage patterns and the average maximum response quantities of the YZ frames: group 1 of accel. (a_g=0.25 g), 30 cm thick foundation slab

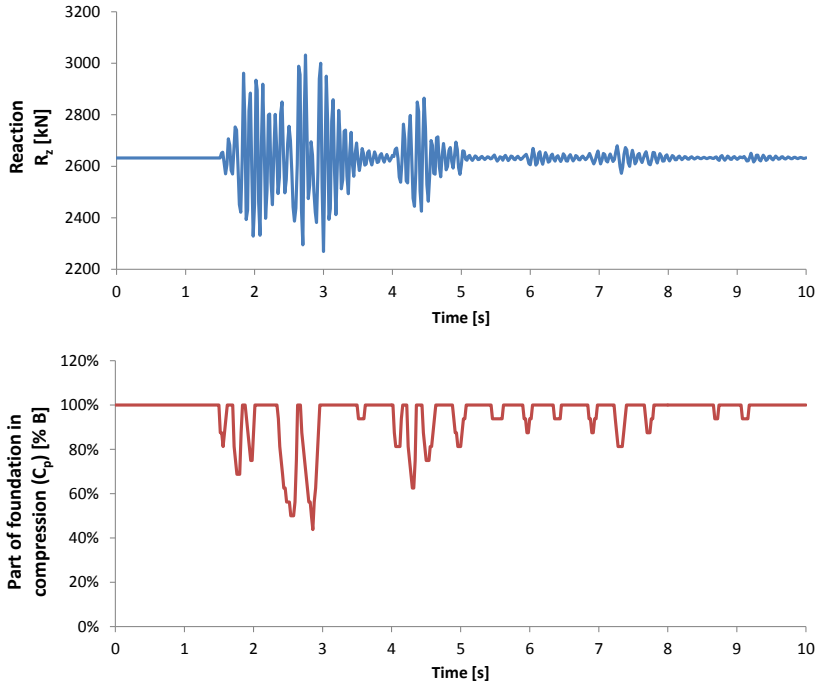

Fig. 16 The time-history response of the model B6-TI-soilA (frame YZ, 30 cm thick foundation slab) subjected to synthesized accel. Banja Luka (a_g=0.25 g)

3.7 The effect of the seismic intensity

In order to investigate the effect of seismic intensity, the B4-TI-soilA frame YZ with an actual (30 cm thick) foundation slab on XPS 400 was also subjected to a stronger earthquake event (a_g=0.35 g). For this purpose the previously used synthesized seven ground motion records were scaled by factor of 1.4. The average absolute displacements and the obtained damage patterns of the frame can be found in (Koren and Kilar 2014). For the sake of brevity, in this paper only the response amplifications are commented upon. Comparing the response under the two analysed seismic intensities (a_g=0.25 g and 0.35 g) for the investigated model, the 40% larger seismic input resulted in 100% larger lateral roof displacements (D_y), whereas the increase in the vertical displacements at the edge of the foundation slab was much smaller (~25%). With respect to the latter, it should be mentioned that also in the case of the higher seismic intensity the obtained maximum compressive deformations in the XPS did not exceed the latter's yield deformation value (2.1% *d*).

4. Conclusions

In principle a thermal insulation (TI) layer installed beneath a building acts similarly to a seismic base isolation system since it elongates the structural period. However, TI/FB amplifications (structures with vs. structures without TI beneath the foundation slab) of the fundamental period are much smaller in comparison to those observed in the case of structures that

are base-isolated by means of seismic isolation devices. In the case of the TI models it was observed that there were significant amplifications in the accelerations that were transferred from the soil to the top of the ground floor slab. It should be noted that such a response is quite different to the response of structures that are base-isolated by means of seismic isolation devices. In the presented study medium-height symmetric RC frame buildings with fundamental periods in the resonance part of the acceleration response spectrum were selected as being critical test structures. Based on the results obtained, the following conclusions have been made, which should, however, be limited to the analysed buildings founded on a TI layer made of extruded polystyrene (XPS):

• The results showed that the use of TI beneath the foundation slab of a superstructure generally induces a higher structural peak response compared to the system where there is no TI beneath the foundation slab. These response amplifications could be substantial and might result in the exceedance of the structural or TI layer capacity values. For the analysed TI variants of the superstructure which was previously designed as a FB variant in accordance with the seismic codes it was shown that, in the case of a design earthquake load, the response amplifications do not necessarily result in substantial exceedance of the ultimate limit states. In the analysed cases unfavourable damage patterns (partial collapse mechanisms) were observed only in the case of buildings with TI beneath the foundation slab.

• During an earthquake the uplift of a building's foundation slab on a XPS layer is a likely response in the case of slender buildings (with larger height-to-width ratios) whose response is governed mainly by the rocking mode of oscillation, and have a higher tendency to overturn.

• In order to prevent possible uncontrolled horizontal sliding between the different foundation layers of the building (i.e., concrete, TI, waterproofing sheet, etc.) appropriate foundation sets with sufficient friction capacity need to be used. From the point of view of friction demand, special attention should be paid in the case of low-rise (2-storeyed) and light-weight buildings.

• It is recognized that the incorporation of soil-structure interaction (SSI) may have a significant impact on the structural dynamic response. The TI/FB response amplifications assume the largest values in the case of foundations on firm soils. In the case of buildings founded on poor soil conditions, the effect of soft soil prevails and the response of the FB and TI models is almost the same. However, the largest overall response in terms of the absolute values of the response quantities was obtained in the case of models founded on poor soil.

• Analysis of the foundation slab stiffness effect showed that the response of the superstructure, as well as that of the XPS, is substantially affected by the stiffness of the foundation slab (especially in the case of multi-bay frames). In the case analysed in this paper, the XPS edge stresses under the rigid foundation slab were underestimated by as much as a factor of 2 in comparison with the corresponding stresses obtained in the case of a foundation slab with actual (30 cm thick) stiffness. If accurate seismic analysis of a building is to be performed, the actual stiffness of the foundation slab should be taken into account.

• The XPS vertical (compressive) deformability and strength was shown to be the main XPS parameter which affects the structural dynamic response, whereas the corresponding XPS shear characteristics did not significantly affect the response. The largest demands for the XPS layer in terms of compressive deformation were obtained in the case of stiff and slender medium-height (6-storeyed) buildings.

• In the study a simplified analysis of two characteristic 2D frames has been performed. It should be noted that, in the case of a real complex 3D building model, the stresses and deformations of the XPS layer at the corners of the foundations could be larger than those obtained in the case of the 2D models used in the study.

Acknowledgments

The financial support from the Slovenian Research Agency (Project *No. L5-4319* and Program *No. P5-0068*) is hereby gratefully acknowledged, as well as that of the project's other co-funders (The Building and Civil Engineering Institute ZRMK and the companies FIBRAN NORD, DULC and BAZA ARHITEKTURA).

References

Ambraseys, N., Smit, P., Sigbjornsson, R., Suhadolc, P. and Margaris, B. (2002), *Internet-Site for European Strong-Motion Data* (http://www.isesd.hi.is/ESD_Local/frameset.htm), European Commission, Research-Directorate General, Environment and Climate Programme.

Anagnostopoulos, S.A., Kyrkos, M.T. and Stathopoulos, K.G. (2015), "Earthquake induced torsion in buildings: critical review and state of the art", *Earthq. Struct.*, **8**(2), 305-377.

Apostolou, M., Gazetas, G. and Garini, E. (2007), "Seismic response of slender rigid structures with foundation uplifting", *Soil Dyn. Earthq. Eng.*, **27**(7), 642-654.

Azinović, B., Koren, D. and Kilar, V. (2014a), "The seismic response of low-energy buildings founded on a thermal insulation layer - A parametric study", *Eng. Struct.*, **81**, 398-411.

Azinović, B., Koren, D. and Kilar, V. (2014b), "Principles of energy efficient construction and their influence on the seismic resistance of light-weight passive buildings", *Open Civ. Eng. J.*, **8**, 105-116.

Bhattacharya, K. and Dutta, S.C. (2004), "Assessing lateral period of building frames incorporating soil-flexibility", *J. Sound Vib.*, **269**(3-5), 795-821.

Bunge, F. and Merkel, H. (2011), "Development, testing and application of extruded polystyrene foam (XPS) insulation with improved thermal properties", *Bauphysik*, **33**(1), 67-72.

CEN (2004), *European standard EN 1990 - Eurocode 0 - Basis of structural design*, European Committee for Standardization, Brussels.

CEN (2005a), *European standard EN 1998-1 - Eurocode 8, Design of structures for earthquake resistance - Part 1: General rules, seismic actions and rules for buildings*, European Committee for Standardization, Brussels.

CEN (2005b), *European standard EN 1997-1 - Eurocode 7, Geotechnical design - Part 1: General rules*, European Committee for Standardization, Brussels.

Cheraghi, R.E. and Izadifard, R.A. (2013), "Demand response modification factor for the investigation of inelastic response of base isolated structures", *Earthq. Struct.*, **5**(1), 23-48.

CSI (2011), *SAP2000 Ultimate (v15.0.0) - Structural Analysis Program*, Computer & Structures, Inc., Berkeley, California, USA.

Dequaire, X. (2012), "Passivhaus as a low-energy building standard: contribution to a typology", *Energy Effic.*, **5**(3), 377-391.

Dolšek, M. and Fajfar, P. (2007), "Simplified probabilistic seismic performance assessment of plan-asymmetric buildings", *Earthq. Eng. Struct. Dyn.*, **36**(13), 2021-2041.

Feist, W. (1996), "Life-cycle energy balances compared: low-energy house, passive house, self-sufficient house", *Proceedings of the international symposium of CIB W67*, Vienna, Austria.

Feist, W. (2007), *Wärmebrücken und Tragwerksplanung - die Grenzen des wärmebrückenfreien Konstruierens, Protokollband Nr. 35*, Passivhaus Institut, Darmstadt.

Gazetas, G. (1991), "Formulas and charts for impedances of surface and embedded foundations", *J. Geotech. Eng., Am. Soc. Civ. Eng.*, **117**(9), 1363-1381.

Gelagoti, F., Kourkoulis, R., Anastasopoulos, I. and Gazetas, G. (2012), "Rocking isolation of low-rise frame structures founded on isolated footings", *Earthq. Eng. Struct. Dyn.*, **41**(7), 1177-1197.

Ghannad, M.A. and Jafarieh, A.H. (2014), "Inelastic displacement ratios for soil-structure systems allowed to uplift", *Earthq. Eng. Struct. Dyn.*, **43**(9), 1401-1421.

Giarlelis, C., Lekka, D., Mylonakis, G. and Karabalis, D.L. (2011), "The M6.4 Lefkada 2003, Greece, earthquake: dynamic response of a 3-storey R/C structure on soft soil", *Earthq. Struct.*, **2**(3), 257-277.
Iervolino, I., Galasso, C. and Cosenza, E. (2010), "REXEL: computer aided record selection for code-based seismic structural analysis", *Bull. Earthq. Eng.*, **8**(2), 339-362.
Islam, A.B.M.S., Hussain, R., Jumaat, M.Z. and Rahman, M.A. (2013b), "Nonlinear dynamically automated excursions for rubber-steel bearing isolation in multi-storey construction", *Automat. Constr.*, **30**, 265-275.
Islam, A.B.M.S., Jumaat, M.Z., Hussain, R. and Alam, M.A. (2013a), "Incorporation of rubber-steel bearing isolation in multi-storey building", *J. Civ. Eng. Manag.*, **19**(Supplement 1), S33-S49.
Jarernprasert, S., Bazan-Zurita, E. and Bielak, J. (2012), "Seismic soil-structure interaction response of inelastic structures", *Soil Dyn. Earthq. Eng.*, **47**, 132-143.
Kilar, V. and Koren, D. (2009), "Seismic behaviour of asymmetric base isolated structures with various distributions of isolators", *Eng. Struct.*, **31**(4), 910-921.
Kilar, V., Koren, D. and Bokan Bosiljkov, V. (2014), "Evaluation of the performance of extruded polystyrene boards - implications for their application in earthquake engineering", *Polym. Test.*, **40**, 234-244.
Kilar. V., Koren, D. and Zbašnik-Senegačnik, M. (2013), "Seismic behaviour of buildings founded on thermal insulation layer", *Građevinar*, **65**(5), 423-433.
Koren, D. and Kilar, V. (2011), "The applicability of the N2 method to the estimation of torsional effects in asymmetric base-isolated buildings", *Earthq. Eng. Struct. Dyn.*, **40**(8), 867-886.
Koren, D. and Kilar, V. (2014), "Buildings founded on thermal insulation layer subjected to earthquake load", *Int. J. Civ., Arch., Struct., Constr. Eng.*, **8**(5), 49-57.
Koren, D., Kilar, V. and Zbašnik-Senegačnik, M. (2013), "Seismic safety of passive houses founded on thermal insulation", *Proceedings of the 17th International Passive House Conference 2013*, Frankfurt am Main, Germany.
Kreslin, M. and Fajfar, P. (2010), "Seismic evaluation of an existing complex RC building", *Bull. Earthq. Eng.*, **8**(2), 363-385.
Kuzman, M.K., Grošelj, P., Ayrilmis, N. and Zbašnik-Senegačnik, M. (2013), "Comparison of passive house construction types using analytic hierarchy process", *Energy Build.*, **64**, 258-263.
Mahmoud, S., Austrell, P.-R. and Jankowski, R. (2012), "Simulation of the response of base-isolated buildings under earthquake excitations considering soil flexibility", *Earthq. Eng. Eng. Vib.*, **11**(3), 359-374.
Makris, N. (2014), "A half-century of rocking isolation", *Earth. Struct.*, **7**(6), 1187-1221.
Merkel, H. (2004), "Determination of long-term mechanical properties for thermal insulation under foundations", *Proceedings of the Buildings IX Conference*, ASHRAE, Atlanta, USA.
Moghaddasi, M., MacRae, G.A., Chase, J.G., Cubrinovski, M. and Pampanin, S. (2015), "Seismic design of yielding structures on flexible foundations", *Earthq. Eng. Struct. Dyn.*, **44**(11), 1805-1821.
Mylonakis, G. and Gazetas, G. (2000), "Seismic soil-structure interaction: beneficial or detrimental?", *J. Earthq. Eng.*, **4**(3), 277-301.
Naeim, F. and Kelly, J.M. (1999), *Design of Seismic Isolated Structures, From Theory to Practice*, John Wiley & Sons Inc., New York, NY, USA.
Naumoski, N.D. (1998), *Program SYNTH: Generation of Artificial Accelerograms Compatible with Target Spectrum*.
Ohara, Y., Tanaka, K., Hayashi, T., Tomita, H. and Motani, S. (2004), "The development of a non-fluorocarbon-based extruded polystyrene foam which contains a halogen-free blowing agent", *Bull. Chem. Soc. Japan*, **77**(4), 599-605.
Paulay, T. and Priestley, M.J.N. (1992), *Seismic Design of Reinforced Concrete and Masonry Buildings*, John Wiley & Sons Inc., New York, NY, USA.
Praznik, M., Butala, V. and Zbašnik-Senegačnik, M. (2013), "Simplified evaluation method for energy efficiency in single-family houses using key quality parameters", *Energy Build.*, **67**, 489-499.
Proietti, S., Sdringola, P., Desideri, U., Zepparelli, F., Masciarelli, F. and Castellani, F. (2013), "Life cycle assessment of a passive house in a seismic temperate zone", *Energy Build.*, **64**, 489-499.
Sadek, E. and Fouad, N.A. (2013), "Finite element modeling of compression behavior of extruded

polystyrene foam using X-ray tomography", *J. Cell. Plast.*, **49**(2), 161-191.
Sykora, D.W. (1987), *Examination of existing shear wave velocity and shear modulus correlations in soils: Final Report AD-A214 721*. US Army Engineer Waterways Experiment Station, Corps of Engineers, Geotechnical Laboratory, Mississippi.
Varnava, V. and Komodromos, P. (2013), "Assessing the effect of inherent nonlinearities in the analysis and design of a low-rise base isolated steel building", *Earth. Struct.*, **5**(5), 499-526.
Vo, C.V., Bunge, F., Duffy, J. and Hood, L. (2011), "Advances in thermal insulation of extruded polystyrene foams", *Cell. Polymers*, **30**(3), 137-155.
Wolf, J.P. (1997), "Spring-dashpot-mass models for foundation vibrations", *Earthq. Eng. Struct. Dyn.*, **26**(9), 931-947.
Wu, W.-H. and Lee, W.-H. (2002), "Systematic lumped parameter models for foundations based on polynomial fraction approximation", *Earthq. Eng. Struct. Dyn.*, **31**(7), 1383-1412.

SA